R-spondin 3 deletion favors Erk phosphorylation to enhance Wnt signaling and bone formation

Kenichi Nagano
Harvard School of Dental Medicine and Harvard Medical School
Kei Yamana
Harvard School of Dental Medicine and Harvard Medical School
Hiroaki Saito
Harvard School of Dental Medicine
Riku Kiviranta
University of Turku
Ana Clara Pedroni
Harvard School of Dental Medicine and Harvard Medical School
Dhairya Raval
Harvard School of Dental Medicine and Harvard Medical School
Christof Niehrs
German Cancer Research Centre (DKFZ)
Francesca Gori (francesca_gori@hsdm.harvard.edu)
Harvard School of Dental Medicine and Harvard Medical School
Roland Baron
Department of Medicine, Harvard Medical School https://orcid.org/0000-0001-5784-5934

Article

Keywords: R-spondin 3, skeletal homeostasis, Erk signaling, Wnt signaling.

Posted Date: June 21st, 2021

DOI: https://doi.org/10.21203/rs.3.rs-569623/v1

R-spondin 3 deletion favors Erk phosphorylation to enhance Wnt signaling and bone formation.

Kenichi Nagano[1], Kei Yamana[1], Hiroaki Saito[1], Riku Kiviranta[1], Ana Clara Pedroni[1], Dhairya Raval[1], Christof Niehrs[2, 3], Francesca Gori[1*] and Roland Baron[1,4*].

[1]Division of Bone and Mineral Research, Harvard School of Dental Medicine and Harvard Medical School, [2]Division of Molecular Embryology, DKFZ-ZMBH Alliance, Deutsches Krebsforschungszentrum (DKFZ), 69120, Heidelberg, Germany, [3] Institute of Molecular Biology (IMB), 55128, Mainz, Germany, [4]Endocrine Unit, Massachusetts General Hospital.

*Co-senior Authors

Key Words: R-spondin 3, skeletal homeostasis, Erk signaling, Wnt signaling.

Address correspondence to:

Francesca Gori
Division of Bone and Mineral Research
Department of Oral Medicine, Infection and Immunity
Harvard School of Dental Medicine
Boston, MA 02115
Tel: (617) 432-1940
Fax: (617) 432-1897
Email: francesca_gori@hsdm.harvard.edu

And

Roland Baron
Division of Bone and Mineral Research
Department of Oral Medicine, Infection and Immunity
Harvard School of Dental Medicine
Boston, MA 02115
Tel: (617) 432-7320
Fax: (617) 432-1897
Email: roland_baron@hsdm.harvard.edu

Abstract

Activation of Wnt signaling leads to high bone density. The R-spondin family of four secreted glycoproteins (Rspo1-4) amplifies Wnt signaling. In humans, RSPO3 variants are strongly associated with bone density, but how RSPO3 affects skeletal homeostasis is not fully understood. Here we show that in mice *Rspo3* haplo-insufficiency or its targeted deletion in osteoprogenitors lead to an increase in bone formation and bone mass. Contrary to expectations, *Rspo3* haplo-insufficiency results in canonical Wnt signaling activation. Using mouse embryonic fibroblasts we show that *Rspo3* deficiency leads to activation of Erk signaling, stabilizing β-catenin. Furthermore, *Rspo3* haplo-insufficiency impairs Dkk1 efficacy in blocking canonical Wnt signaling and prevents the *in vivo* inhibition of bone formation and bone mass induced by osteoblast-targeted expression of *Dkk1*. We conclude that *Rspo3* haplo-insufficiency/deficiency boosts canonical Wnt signaling by activating Erk signaling and impairing Dkk1's inhibitory activity, which in turn lead to increased bone formation and bone mass.

Introduction

The Wnt signaling pathway controls cell fate decisions and tissue homeostasis during development and in the adult [1,2]. It is also involved in skeletal development and essential for the regulation of bone mass in the adult skeleton [3-5]. Genetic or therapeutic activation of canonical Wnt signaling is associated with increased bone mass [3] and current therapeutic approaches aim at activating this pathway in patients with osteoporosis or osteogenesis imperfecta for instance [6].

Wnt signaling involves a large number of receptors and co-receptors, and of endogenous agonists and antagonists that, together, tightly regulate its activation (1-4). Due to this complexity, and even though Wnt signaling has been studied extensively in recent years in bone, several aspects of the mechanisms by which it regulates bone mass remain unclear. Similarly, the specific downstream events regulated by these various components of the Wnt signaling machinery and their interaction with other signaling cascades remain puzzling.

In this context, the fact that several studies have demonstrated that the four Roof plate-specific spondin, R-spondins (Rspo1 to 4), synergize with Wnt ligands to activate Wnt signaling [4,7-13] raises the question of their potential role in skeletal development and homeostasis. This enhancement of Wnt activity is attributed to the ability of Rspos to prevent the ubiquitination and degradation of the Lrp5/6/Fzd receptor complex via Lgr4-6, closely related orphans of the leucin-rich repeat containing G protein-coupled receptors, and the transmembrane E3 ubiquitin ligases ring finger 43 (Rnf43) and zinc and ring finger 3 (Znrf3), sensitizing cells to Wnt ligands [7,14-18]. Although the role of Lgr receptors in the effects of Rspos is well established, recent reports have shown that Rspo2 and Rspo3 can also enhance Wnt signaling independently of Lgr receptors, possibly by acting as direct antagonist ligands to RNF43 and ZNRF3 [11,19,20].

Of particular interest is the fact that, in contrast to the many studies that have reported that Rspos co-activate Wnt signaling, some studies in Zebrafish have indicated that Rspo3 can also function as a negative regulator of canonical Wnt signaling during dorsoventral and anteroposterior patterning [21,22]. Additionally, it has been shown that Rspos can potentiate non-canonical Wnt cascades, such as the Wnt/PCP signaling [14,15] and can function as antagonists of BMPR1 in *Xenopus* [23], two events that could have a negative impact on bone formation and bone mass. Thus, the mechanisms involved in the Rspos/Wnt signaling axis and their influence on skeletal homeostasis appear be more complex *in vivo*.

The four Rspos belong to a family of cysteine-rich secreted glycoproteins with high structural similarity and 60% sequence homology [8,11]. Although all Rspos are expressed in bone during development, they appear to have specific functions and their deletion in mice and human leads to different phenotypes [10,13,24-31]. Within the Rspo family, Rspo3 is of particular interest for bone because it is highly expressed in skeletal elements during development [32] and several human GWA studies have shown that RSPO3 SNPs are strongly associated with bone mineral density and risk of fracture [33-38]. Not surprisingly, *in vitro* studies have shown that overexpression of, or treatment with, Rspos can enhance Wnt-ligand mediated osteoblast (OB) differentiation [10,28,39]. However, it has also been

reported that Rspo3 may function as a negative regulator of osteoblast differentiation [40], raising questions about the true net influence of Rspos, and in particular Rspo3, on skeletal homeostasis.

Thus, despite the consensus that Rspos co-activate Wnt signaling, Rspo3 may play a specific role in skeletal biology and disease, exerting a positive and/or a negative influence on bone. Little is known about its specific effects and on the mechanisms by which Rspo3 affects the skeleton *in vivo.* Here, we show that, in mice, decreasing the levels of Rspo3 increases Erk phosphorylation, activates Wnt signaling and is anabolic to bone*,* suggesting that its specific inhibition could constitute a therapeutic mean to increase bone mass.

Results

Rspo3 haplo-insufficiency increases bone formation and trabecular bone mass.

Rspo3 is expressed in bones during skeletal development [32]. We assessed *Rspo3* mRNA levels in primary calvarial osteoblasts (cOBs) and found that it is expressed in these cells and that its expression increases significantly during OB differentiation (Fig. S1a). To determine the physiological role of Rspo3 in skeletal homeostasis, we first used mice in which *Rspo3* has been germline-deleted [27]. As global deletion of *Rspo3* leads to lethality by E9.5 [24,27], before skeletal development, we analyzed mice lacking only one *Rspo3* allele. *Rspo3*$^{+/-}$ mice develop normally (Fig. S1b), are fertile and are born at the expected Mendelian ratio. These mice continue to be healthy and do not develop any particular pathology as they age (up to one year) (data not shown). Most surprisingly however, and contrary to expectations, two-way ANOVA analysis of the skeletal phenotype at 6, 12 and 18-week (wk) of age, revealed highly significant ($p<0.001$) anabolic effects of *Rspo3* haplo-insufficiency on structural, cellular and dynamic parameters in both female and male mice (Fig.1a, Table 1, Table S1 and Fig. S1c). The skeletal phenotype of *Rspo3*$^{+/-}$ male and female mice is overall characterized by an increase in trabecular bone mass with high bone formation, mineral apposition rate and OB number and surface whereas bone resorption parameters are not affected (Fig.1a, Table 1,Table S1 and Fig. S1c). As expected, the two-way ANOVA also demonstrated an effect of age, affecting

primarily the structural parameters (Fig. 1a, Table 1 and Table S1). At 12 wk of age *Rspo3* haplo-insufficiency led to a significant increase in trabecular bone mass (BV/TV), trabecular thickness (Tb.Th.) and trabecular number (Tb.N) (Fig. 1b and 1d, Table 1 and Table S1). In both genders bone resorption parameters (Oc.S/B.Pm and N.Oc/B.Pm) were not changed in Rspo3$^{+/-}$ mice. In contrast, *Rspo3*$^{+/-}$ mice exhibited an increase in bone formation parameters (BFR/BS) (Fig. 1b-d, Table 1 and Table S1). The increase in BFR was associated with an increase in mineral apposition rate (MAR), indicating a marked increase in the activity of individual OBs in *Rspo3*$^{+/-}$ mice, in addition to the increase in their numbers (N.Ob/B.pm, Fig. 1d, Table 1 and Table S1). Consistent with these results, the osteoid surface (OS/BS) and the OB surface (Ob.S/B.Pm) were also significantly increased in both genders (Table 1 and Table S1). Despite these marked effects on trabecular bone, all cortical bone parameters were unchanged in *Rspo3*$^{+/-}$ female and male mice at 12 wk of age (Fig. 1d, Table S2 and S3), indicating that *Rspo3* haplo-insufficiency affects preferentially trabecular bone homeostasis.

Thus, in contrast with the expectation that decreasing the expression of a Wnt signaling potentiator might lead to a decrease in bone formation and bone mass, our data clearly indicates that *Rspo3* haplo-insufficiency induces an increase in trabecular bone mass due to a significant increase in bone formation, with no changes in bone resorption. In agreement with our *in vivo* observations, we found that, although *Rspo3* is expressed in bone marrow macrophage (BMM)-derived osteoclasts (OCs) (Fig. S2a), there was no significant differences in the formation of TRAP^{+} multinucleated cells and in the expression of OC marker genes (*Ctsk*, *Trap*, *Nfatc1*) between BMM cultures from *wt* and *Rspo3*$^{+/-}$ mice in response to M-CSF and RANKL (Fig. S2b and 2Sc). In addition, mix-and-matched co-cultures of cOBs and BMMs from *wt or Rspo3*$^{+/-}$ mice confirmed that *Rspo3* haplo-insufficiency does not affect osteoclastogenesis, whether directly or indirectly (Fig. S2d).

***Rspo3* haplo-insufficiency leads to an increase in bone marrow precursor cells and in their osteoblast potential.**

Given that the OB number was significantly increased in mutant mice (Fig. 1, Table 1 and Table S1) we hypothesized an increase in the population of precursor cells. Bone marrow flow cytometry showed that while the total number of bone stromal cells (Lin^-CD45^-) was not significantly affected by Rspo3 haplo-insufficiency (4047±1245 in *wt* compared to 5867+2382 in $Rspo3^{+/-}$, mean ± SEM n=10), the mesenchymal stromal cells (MSC) population (defined here as $Lin^-CD45^-CD31^-CD51^+Sca\text{-}1^+$) was significantly increased in $Rspo3^{+/-}$ mice compared with *wt* littermates (Fig. 2a and 2b) [41]. Consistent with these findings and with the observed increase in OB number and bone formation, Rspo3 haplo-insufficiency significantly increased CFU-F and CFU-OB formation (Fig. 2c). These data show that the changes induced by *Rspo3* haplo-insufficiency affect the bone marrow MSC lineage and induce an increase in the pool of progenitor cells with an osteoblast potential.

Specific deletion of *Rspo3* in cells of the osteoblast lineage mirrors the skeletal phenotype seen with global *Rspo3* haplo-insufficiency.

To assess whether the effect on bone mass seen in *Rspo3* haplo-insufficient mice was cell-autonomous to cells of the OB lineage, we generated mice with deletion of *Rspo3* in OB precursors ($Rspo3^{OB}$) by crossing $Rspo3^{fl/fl}$ mice with *Runx2Cre* mice [42]. OB lineage-targeted deletion of *Rspo3* (Fig. 3a) mirrored the skeletal phenotype seen in $Rspo3^{+/-}$ mice as indicated by a significant increase in BV/TV, MAR, BFR/BS, OS/BS and N.Ob/B.Pm in $Rspo3^{OB}$ compared to their control ($Rspo3^{fl}$) male and female littermates. Once again there was no changes in OC parameters (Fig. 3b, 3c and Table S4). These findings indicate that the increase in bone formation and in bone mass results from a cell-autonomous effect of *Rspo3* insufficiency in osteoblast progenitors.

***Rspo3* haplo-insufficiency and deletion lead to β-catenin stabilization.**

The above results raised the question of how reduction in *Rspo3*, classically considered a potentiator of canonical Wnt signaling, leads to increased bone formation and trabecular bone mass. To address this question, we first looked at the status of the Wnt signaling pathway in *Rspo3* haplo-

insufficiency. Surprisingly, but consistent with the observations on bone formation, *Rspo3* haplo-insufficiency led to a remarkable increase in the expression of the canonical Wnt target genes *Dkk1, Axin2* and *Opg* in marrow-flushed long bones and in the protein levels of activated β-catenin (Fig.4a and 4b). Importantly, we noted no difference in the mRNA levels of *Rspo1* and *Rspo2* between *Rspo3*$^{+/-}$ and *wt* marrow-flushed long bones (Fig.4a). We also observed that *Sost* expression was, in contrast with that of *Dkk1*, not affected by *Rspo3* haplo- insufficiency suggesting that the bone formation and Wnt signaling changes seen in *Rspo3*$^{+/-}$ mice are independent of sclerostin levels (Fig.4a). While both *Opg* and *Rankl* expression was increased, the *Rankl/Opg* ratio remained unchanged in *Rspo3*$^{+/-}$ long bones, consistent with our *in vivo* and *in vitro* observation of unchanged number of OCs. Given the observed increase in OB progenitors in the bone marrow of *Rspo3*$^{+/-}$ mice (Fig. 2), we also determined the level of Wnt signaling activation in *Rspo3* haplo-insufficient bone marrow MSCs (BMSCs). Canonical Wnt signaling was also activated in these cells, as indicated by increased expression of several canonical Wnt target genes and increased active β-catenin levels (Fig. 5a and 5b). Thus, surprisingly but consistent with the bone and OB phenotypes, *Rspo3* haplo-insufficiency leads to activation of canonical Wnt signaling, which in turn results in increased bone formation.

To exclude any function of the remaining Rspo3 on canonical Wnt signaling in the *Rspo3*$^{+/-}$ mice and cells, we generated *Rspo3*$^{-/-}$ mouse embryonic fibroblasts (MEFs) at E9.5, before embryonic lethality [24,27]. As shown by several groups [7,8,12,29], we confirmed that while Rspo3 does not activate Wnt signaling by itself, it potentiates exogenous Wnt3a action in *wt* MEFs as indicated by the Tcf-1/Lef luciferase reporter assay (Fig. 6a). Counter-intuitively, *Rspo3* deficiency led to a marked increase in the expression of the canonical Wnt target genes *Tcf-1 and Axin2* at steady-state (Fig. 6b) as well as to a significant increase in the levels of pLrp6, activated β-catenin and Tcf-1 (Fig 6c). Accordingly, TOPflash reporter activity was significantly increased in *Rspo3* null MEFs compared to *wt* MEFs and further increased by Wnt3a treatment (Fig. 6d). Similarly, upon Wnt3a treatment, *Axin2*

and *Tcf-1* expression as well as pLrp6 and activated β-catenin levels, were increased in the absence of *Rspo3* (Fig. 6c-d). Thus, these findings confirm that, unexpectedly, haplo-insufficiency and absence of *Rspo3* in BMSCs and MEFs respectively lead to β-catenin stabilization and enhancement of β-catenin-dependent signaling. We then explored the mechanisms by which Rspo3 may regulate Wnt signaling.

***Rspo3* haplo-insufficiency and deletion impair Dkk1-Wnt inhibitory activity.**

Activation of canonical Wnt signaling results from changes in endogenous activators and/or inhibitors levels and/or activity. Interestingly, we found that Wnt3a decreases the expression of *Rspo3* in *wt* MEFs, whereas it is significantly increased by Dkk1 (Fig. 7a). This raised the possibility that Rspo3 participates in a feedback loop that tones down or balances canonical Wnt activity. Our results below suggest that the reduction in *Rspo3* levels induced by Wnt3a may enhance Wnt signaling by decreasing Dkk1 Wnt inhibitory activity. Indeed, as shown in Figure 7b, the ability of Dkk1 to block Wnt3a-dependent activation of canonical Wnt signaling was significantly impaired in the absence of *Rspo3*: whereas in *wt* MEFs, 50% reduction in the reporter activity was achieved by 50 ng/mL Dkk1, a dose of 400 ng/mL Dkk1 (8x higher) was needed to obtain the same level of inhibition in *Rspo3* null MEFs (Fig. 7b). A similar difference was also observed in pLrp6 and β-catenin protein levels (Fig. 7c). To determine whether this relationship between Rspo3 levels and Dkk1 efficacy was also happening *in vivo*, we crossed *Rspo3*$^{+/-}$ mice with mice expressing high levels of Dkk1 in OBs *(Dkk1-Tg* mice), which exhibit impaired canonical Wnt signaling and low trabecular bone mass due to decreased bone formation [43]. Histomorphometric analysis showed that the low BV/TV and decreased bone formation parameters (MAR, BFR/BS and N.Ob/B.pm) seen in *Dkk1-Tg* mice were significantly rescued by *Rspo3* haplo-insufficiency (Fig. 7d, 7e and Table S5). These data, together with the findings that *Dkk1* expression is higher in *Rspo3*$^{+/-}$ long bone, despite the fact that *Rspo3*$^{+/-}$ mice display higher trabecular bone mass, indicate that *Rspo3* haplo-insufficiency counteracts the effect of Dkk1 overexpression on the skeleton.

***Rspo3* deletion enhances Erk signaling, increasing pLrp6 and stabilizing β-catenin.**

Since both *Rspo3* haplo-insufficiency and its deletion lead to β-catenin stabilization, we then asked whether, possibly in addition to or explaining the decreased efficacy of Dkk1, Rspo3 might also be involved in the regulation of other signaling pathways which in turn can stabilize β-catenin, stimulating osteoblastogenesis and counteracting Dkk1 efficacy. It has been proposed that Rspo3 binding to Lgr4 inhibits Erk phosphorylation (pErk) [23,40,44]. We therefore investigated Erk signaling, known to activate Wnt signaling and to regulate OB differentiation and bone mass [45-48], in our model. *Rspo3* deficiency led to a clear and significant increase in pErk basal levels (Fig. 8a). Although in *wt* cells the specific Erk inhibitor U0126 significantly decreased both the basal and the Wnt3a-dependent increase in pErk, it did not significantly affect active β-catenin levels. In contrast, inhibition of pErk in *Rspo3*$^{-/-}$ cells led to a significant decrease in active β-catenin levels in both steady state and Wnt3a-stimulated cultures. A similar effect was also seen for the levels of pLrp6 (Fig. 8a). Confirming these findings, the increase in the expression of the canonical Wnt signaling target genes *Tcf1* and *Axin2* was also partially rescued by blocking Erk signaling in Rspo3 null MEFs (Fig. 8b). Thus, the stabilization of β-catenin we observe in the absence of Rspo3 is due, at least in part, to activation of the Erk pathway.

Discussion

Wnt signaling is central to skeletal development and homeostasis in health and disease [3]. Understanding the biological mechanisms by which this signal operates is therefore of both scientific and clinical interest. R-Spondins, classically considered as positive modulators of Wnt signaling, play an important role in normal development of several tissues and organs including bone, and are implicated in human diseases [8,9,11-13]. Investigating further their exact function therefore holds therapeutic potential. Our results clearly demonstrate, through several independent lines of genetic *in vivo* and *in vitro* experiments, that, counter-intuitively, decreasing *Rspo3* results in canonical Wnt signaling activation, increased bone formation and high bone mass. This response is mainly driven by

increased number of OB progenitors and OBs as well as an increase in their bone forming activity, with no effect on OC number and bone resorption. Thus, our studies reveal a novel and unexpected negative function of Rspo3 on the Wnt signaling machinery in bone homeostasis. This might have implications for our understanding of the multi-faceted aspects of Wnt signaling regulation of skeletal homeostasis, and possibly reveal novel ways to increase bone mass in patients.

Despite the fact that the four Rspos display high structural similarity and sequence homology, they display differential expression profiles [32] and have unique and distinct functions [8,11,49]. Studies in mice have shown that during embryonic development Rspo3 is highly expressed in the skeleton [32]. Human GWA studies have shown that RSPO3 might be specifically involved in bone metabolism due to the strong association between RSPO3 common variants and bone mineral density [33,34,36-38]. Whether these variants lead to RSPO3 gain of- or loss of- function is however not known. Rspos are considered to be co-activators of Wnt signaling [3,7,29]. Accordingly, treatment with Rspos has been reported to have a positive effect on osteogenesis [10,28,39], such that decreasing its expression levels should have a negative impact on skeletal homeostasis. In contrast, we show here that Rspo3 haplo-insufficiency has an anabolic effect on bone. Importantly, targeted deletion of *Rspo3* in the OB lineage in mice mimicked the skeletal phenotype seen with *Rspo3* global haplo-insufficiency, revealing an OB lineage cell-autonomous effect of Rspo3 in the regulation of skeletal homeostasis.

In vitro studies have demonstrated that overexpression of and treatment with Rspo1 or Rspo2 enhance Wnt ligand-mediated OB differentiation [9,10,28]. Nonetheless, our *in vitro, ex vivo* and *in vivo* studies demonstrate that *Rspo3* haplo-insufficiency and its deletion result in canonical Wnt signaling activation. As discussed later, and although paradoxical, these two observations are not mutually exclusive or discrepant. The literature and our own *in vitro* studies indeed confirm that Rspo3 is, as expected, a co-activator of canonical Wnt signaling in the Topflash assay, potentiating Wnt3a-dependent activation of canonical Wnt signaling in cellular assays ([49] and Fig. 6). Surprisingly however, the expression of canonical Wnt target genes and the levels of pLrp6 and activated β-catenin were markedly increased in *Rspo3* haplo-insufficient bones and BMSCs and in *Rspo3*-null

MEFs, indicating that, counter-intuitively, the decrease or absence of *Rspo3* in bone activates mechanisms that favor β-catenin-dependent signaling.

The findings that *Rspo3* is strongly repressed by Wnt3a and increased by Dkk1, suggest that Rspo3 may in fact provide a negative feedback-loop helping to dampen canonical Wnt activity by repressing Erk phosphorylation (see below). Interestingly, and again confirming activation of the canonical Wnt signaling pathway, the expression of *Dkk1* is also strongly increased by *Rspo3* haplo-insufficiency and depletion, establishing another Rspo3-dependent negative feedback loop. Although the increase in *Dkk1* would be expected to block Wnt activation, we found that Dkk1 efficacy in blocking Wnt3a-dependent activation of canonical Wnt signaling is significantly impaired in the absence of *Rspo3*. Additionally, our finding that *Rspo3* haplo-insufficiency antagonizes the inhibition of bone formation induced by OB-targeted expression of Dkk1 confirms *in vivo* the fact that *Rspo3* haplo-insufficiency counteracts Dkk1 function. The question is whether this occurs at the cell surface or is the result of intracellular changes in alternative pathways regulated by Rspo3. In fact, our findings that the Erk signaling pathway is activated and the basal level of pLrp6 enhanced by *Rspo3* depletion suggests the possibility that the activation of the Wnt signaling pathway results from intra-cellular changes. Alternatively, *Rspo3* haplo-insufficiency and deletion might induce cell surface changes that favor pLrp6 basal level and/or sensitivity to Dkk1 and/or Wnt ligands. Further studies will be required to investigate these possibilities. Interestingly, Sost levels were not altered by *Rspo3* haploinsufficiency suggesting that the effect of Rspo3 on Dkk1 efficacy and expression represents a specific regulatory mechanism.

Although there is an apparent paradox in that both Rspo3 and its deletion increase β-catenin-dependent signaling, these results can in fact be explained. Our data and that of others [23] suggest that there are alternate Rspo3-mediated signaling mechanisms, separate from the Fzd/Lrp/β-catenin Wnt pathway, including the Wnt/PCP signaling [14,15] and that these events can in turn regulate Wnt

signaling intra-cellularly. Indeed, β-catenin can be stabilized independent of the proximal activation of the canonical Wnt signaling machinery through changes in other signaling pathways [3,48,50].

In fact, we show here that deletion of *Rspo3* enhances Erk signaling which, in turn, stabilizes β–catenin independent of the canonical Wnt signaling receptor complex as shown by the significant increase in Erk phosphorylation observed in the absence of *Rspo3*. In turn, this activation of Erk signaling promotes pLrp6 and β-catenin stabilization and has a positive effect on OB differentiation [45,47,48]. Our finding that the increase in Wnt signaling activation seen in the absence of *Rspo3* is abrogated by blocking Erk signaling strongly suggests that the activation of Erk signaling associated with *Rspo3* deficiency is responsible, at least in part, for the observed Wnt signaling activation.

In agreement with our findings, *in vitro* studies have reported that Rspo3 silencing leads to increased OB differentiation of human adipose-derived stem cells by activating the Erk signaling downstream of Lgr4 [40]. Importantly, although Lgrs function as receptors for Rspos, and Rspos/Lgrs interactions enhance Wnt signaling by inducing the clearance of Rnf43 and Znrf3 [16,17,51], there is strong evidence that Rspos/Lgrs interaction can also activate distinct signaling cascades that can affect bone, including the cAMP/PKA/Creb signaling pathway in Lgr4 null mice [52] and the Erk signaling cascade [40,53-55].

Based on our observations, we propose that Rspo3 has a dual mode of action to regulate canonical Wnt signaling and bone formation. This duality is based on the regulation of two distinct signaling cascades and their crosstalk: Rspo3 functions via both the Lgr/Rnf43/Znrf3 and the Lgr/Erk axes, and while activation of the Lgr/Rnf43/Znrf3 axis boosts Wnt signaling strength by the membrane clearance of Rnf43/Znrf3 and subsequent stabilization of Fzd receptors, binding of Rspo3 to Lgr impairs Erk signaling likely due to the membrane clearance of the Lgr receptors, preventing Erk signaling activation and further stabilization of β–catenin (Fig. 9). Thus, haplo-insufficiency and deletion of Rspo3 would dampen Wnt signaling at the cell surface by preventing the Rnf43/Znrf3 effects while enhancing pLrp6 and β–catenin stabilization intracellularly, via Erk phosphorylation,

which has a more potent effect and overcompensates the decrease in Rspo3-dependent proximal Wnt activation in OBs and their progenitors. Because activation of the Lgr/Rnf43/Znrf3 cascade is not exclusively dependent on Rspo3, deletion of *Rspo3* would only hinder canonical Wnt signaling partially. In contrast, lack of *Rspo3* promotes the Lgr/Erk cascade, which leads to Erk signaling activation, which in turn not only enhances β–catenin stabilization (Fig. 9) but also regulates OB differentiation and bone formation. This model can also explain the observed loss of Dkk1 efficacy in inhibiting Wnt signaling: the Erk-dependent stabilization of β–catenin being independent of proximal Wnt receptor activation, Dkk1 cannot dampen the activation of downstream events as they are independent of the LRP5/6-Fzd receptor complex.

Supporting the fact that Rspo3 can also regulate Wnt-independent pathways, a recent study has suggested that Rspo3 acts as an antagonist to BMPR1A, inhibiting BMP signaling during development [23]. Thus, our observations may be due, at least in part, to changes (activation) in BMP signaling, which in turn could lead to the observed increase in pErk [44]. Although this remains a possibility, it seems unlikely. First, in contrast to our observations here, BMP activation in the adult skeleton has been linked to activation of non-canonical Wnt signaling, increased Sost expression and bone resorption [56,57]. Second, several studies have shown that activation of BMP signaling in the osteoblast lineage has a negative impact on bone formation and bone mass [58-61].

In conclusion, our studies suggest that Rspo3 regulates bone formation through its interaction not only with the Wnt receptor machinery but also with other signaling pathways that affect β–catenin stability. Consequently, if its deletion removes a co-activator of Wnt signaling, potentially decreasing bone formation, it also promotes Erk signaling activation, increasing β–catenin stability sufficiently to enhance bone formation and increase bone mass. Furthermore, because *Rspo3* depletion increases *Dkk1* and Dkk1 increases *Rspo3* expression, this study reveals also a novel feedback Wnt signaling regulatory loop. These findings have important implications for understanding the pleiotropic functions

of Rspos and Wnt signaling in skeletal homeostasis and reveal alternative mechanisms to increase bone mass.

Methods

Animals

Rspo3 mice were provided by Dr. Christof Niehrs (DKFZ-ZMBH Alliance, Germany) [27]. The osteoblast specific Dkk1 transgenic (*Dkk1-tg*) mice were generously provided by Dr. Guo and Dr. Kronenberg (Massachusetts General Hospital, MA, USA). *Runx2Cre* mice were provided by Dr. Tuckermann (Ulm University, Ulm, Germany) [42]. All experiments were performed with age- and gender-matched littermates. All animals are in the C57/Bl6 background and were housed in the Harvard Center for Comparative Medicine and all experimental procedures were approved by the Harvard University Institutional Animal Care and Use Committee.

Skeletal phenotype

For bone histomorphometric analysis, 6 12 or 18 wk-old mice were injected with 20 mg/kg of calcein and 40 mg/kg of demeclocycline (Sigma Aldrich, St. Louis, MO, USA) 6, 8 or 9 day, respectively and 2 day prior to the sacrifice. Bone histomorphometric analysis was performed within the proximal tibia under 200X magnification in a 0.9-mm high and 1.3-mm-wide region where was 200 μm away from the growth plate. The OsteoMeasure analyzing software (Osteometrics) was used to generate and calculate the data. Structural parameters (bone volume fraction (BV/TV), trabecular thickness (Tb.Th), trabecular number (Tb.N), and trabecular separation (Tb.Sp) , Cortical Area, (Ct.A.), Total Area (T.Ar), Marrow Area, (Ma.Ar.), Cortical Bone Volume, (Ct.Bv/TV and) Cortical thickness, (Ct.Th.) were obtained by calculating the average of 2 different measurements from consecutive sections. The structural, dynamic, and cellular parameters were presented according to the standardized nomenclature [62].

Flow Cytometry

Bone marrow was analyzed by flow cytometry as previously described [41]. Briefly, bone marrow cells were flushed from femurs and tibiae of 6-8-wk old *wt* or *Rspo3*$^{+/-}$ mice and washed with Hank's Balanced Salt Solution (HBSS). Residual bone samples were further digested in 3 mg/ml type I collagenase (Worthington) for 1 hour at 37°C and released cells were mixed with flushed bone marrow cells. Cells were stained with LIVE/DEAD® Fixable Aqua Dead Cell Stain Kit (Thermo Fisher Scientific, Waltham, MA, USA), anti-lineage-AF700, anti-CD31-PE, anti-Sca-1-PB, anti-CD45-Cy7APC, and anti-CD51-biotin with streptavidin-APC antibodies (BioLegend). Cells were analyzed on a FACS ARIAII (BD Biosciences) upon exclusion of dead cells.

Bone Marrow Stromal Cells and calvarial osteoblasts

Bone marrow cells were flushed from femurs and tibiae of 6-8 wk-old *wt* or *Rspo3*$^{+/-}$ mice and cultured in DMEM supplemented with 10% fetal bovine serum (FBS) (GIBCO) and 1% penicillin (100 U/ml) and streptomycin (100 µg/ml) for 3 days. Adherent MSCs were counted, re-plated onto at a 5,000/cm^2 density and RNA or protein isolated 3 days later. For colony forming unit assays, flushed bone marrow stromal cells were plated (3X10^6/6 wells) for CFU- (Fibroblast) F and CFU-OB assays. CFU-F was detected by staining with 0.2% crystal violet in 2% ethanol for 1 hour and CFU-OB was detected by alkaline phosphatase activity with Napthol AS-MX, n,n-dimethylformamide and Fast Blue RR salt (Sigma Aldrich, St. Louis, MO, USA). Calvarial OBs were isolated from 1-3-day old pups via serial enzymatic digestions and cultured as previously reported [63].

Mouse Embryonic Fibroblasts (MEFs) Primary Culture

To obtain *wt* and *Rspo3*$^{-/-}$ MEFs*, Rspo3*$^{+/-}$ males and females were crossed and the morning of vaginal plug detection was defined as embryonic day (E) 0.5. At E9.5, whole embryos were isolated, washed in PBS, minced in 0.05% trypsin (GIBCO) followed by incubation at 37C for 10 min. After incubation samples were pipetted to obtain single cell suspension and cells cultured in DMEM supplemented with 10% FBS and 1% penicillin/streptomycin. All the experiments were performed in passage 4 to 6 of *wt* or *Rspo3*$^{-/-}$ MEFs. Cells were treated either 50 or 200 ng/ml of recombinant human Wnt3a, recombinant human Dkk1 (50-400 ng/ml), recombinant human Rspo3 (100 ng/ml) (all

from R&D system) or U0126 (10μM) (Selleckchem). For TOPflash luciferase reporter assay, cells were transiently co-transfected with 400 ng TOPflash-luc reporter plasmid and 10 ng control pCMV-Renilla-luciferase (Promega) using Lipofectamine 2000 (Invitrogen) according to the manufacturers protocol. Cells were subjected to serum starvation in DMEM containing 1% FBS overnight. Cells were subsequently treated with recombinant human Wnt3a in the presence and absence of increasing concentration of Dkk1 for 24 hours followed by luciferase assay using the Dual-Glo Assay system (Promega) according to the manufacturers protocol. Data were normalized by Renilla-firefly activity and presented as fold change compare to control group.

Osteoclast Primary Culture and mix-matched co-cultures

Murine bone marrow macrophages were isolated from bone marrow flushed tibiae and femurs of *wt* and *Rspo3*$^{+/-}$ mice at 6 to 8-wk-old as described previously [63]. Briefly, cells were cultured in complete α-MEM with 30 ng/ml macrophage colony-stimulating factor M-CSF (R&D system) in suspension culture dish to which stromal cells and lymphoid cells cannot adhere, at 37 °C for 2-3 days. For osteoclast generation, cells were cultured in 30 ng/ml M-CSF and 10 ng/ml RANKL (R&D systems). For co-culture experiments, mouse calvarial osteoblasts were isolated from newborn *wt* and *Rspo3*$^{+/-}$ as previously reported [63,64] and seeded in 96-well plates (2.000 cells/well) in complete osteogenic α-MEM containing 100 nM Vitamin D3 and 1 μM prostaglandin E2 (Enzo Life Science). After 3 days, 10,000 BMM from *wt* and *Rspo3*$^{+/-}$ mice at 6 to 8-week-old mice were added per well and cocultured for 9 days in complete osteogenic α-MEM. Tartrate-resistant acid phosphatase (TRAP) staining was performed to evaluate the number of osteoclasts according to the manufacture's protocol (Sigma-Aldrich).

Western Blot Analysis

Five ug of total protein were resolved by SDS-PAGE under reducing conditions. Immunodetection was performed with antibodies specific to: Active β-catenin, phosphorylated (p) Lrp6 , p-Erk, total Erk, Tcf-1, Lrp6 and Tubulin (CST8814, CST2568, CST9101, CST9102, CST2203, CST3395, CST2125,

Cell Signaling Technology) GAPDH and Actin (SC32233 and SC1616, Santa Cruz). Immunoreactivities were assessed using ECL plus kit following the manufacture's protocol (Perkin Elmer). Quantification was performed using Image J. Protein levels were normalized to the levels of housekeeping protein or total protein in within the same sample.

Immunohistochemistry

Paraffin embedded decalcified tibiae were fixed in 10% NBF. Five µm thick longitudinal sections were incubated with antibodies specific to active β-catenin (CST8814, Cell Signaling) at 4°C overnight, treated with TSA-biotin and streptavidin-HRP (Perkin Elmer), as per manufacturer's instructions. Analyses were performed on bones from n=3-4 mice/genotype.

Quantitative-Real Time PCR

Total RNA was isolated from cells using the RNeasy Mini Kit (Qiagen) according to the manufacturer's protocols. Total RNA from cortical bone of *wt* and *Rspo3*$^{+/-}$ mice was extracted using Trizol reagent (Invitrogen) followed by RNeasy Mini Kit (Qiagen) according to the manufacturer's protocols. cDNA was synthesized using iScript cDNA synthesis kit (BIO-RAD) and quantitative real time PCR performed. mRNA levels encoding each gene of interest were normalized for β2M or actin mRNA in the same sample and the relative expression of the genes of interest was determined using the formula of Livak and Schmittgen [65]. Data are presented as fold change relative to *wt* cells or animals.

Statistical Analysis

Data are expressed as the mean ± SEM or ± SD. Statistical analysis was conducted using unpaired two-tail Student's t-test, or two-way ANOVA followed by post-hoc test. The difference was considered as significant at $p<0.05$.

Reference

1 Clevers, H. & Nusse, R. Wnt/beta-catenin signaling and disease. *Cell* **149**, 1192-1205, doi:10.1016/j.cell.2012.05.012 (2012).

2 Nusse, R. & Clevers, H. Wnt/beta-Catenin Signaling, Disease, and Emerging Therapeutic Modalities. *Cell* **169**, 985-999, doi:10.1016/j.cell.2017.05.016 (2017).

3 Baron, R. & Kneissel, M. WNT signaling in bone homeostasis and disease: from human mutations to treatments. *Nat Med* **19**, 179-192, doi:10.1038/nm.3074 (2013).

4 Gori, F., Baron, R. Wnt signaling in skeletal homeostasis and diseases. *Osteoporosis, Fifth Edition. Academic Press. Elsevier*, 257-279 (2021).

5 Huybrechts, Y., Mortier, G., Boudin, E. & Van Hul, W. WNT Signaling and Bone: Lessons From Skeletal Dysplasias and Disorders. *Front Endocrinol (Lausanne)* **11**, 165, doi:10.3389/fendo.2020.00165 (2020).

6 Baron, R., Gori, F. & Leder, B. Z. Sclerostin Inhibition in the Treatment of Osteoporosis. *Osteoporosis*

Pathophysiology and Clinical Management. Editors: Leder BZ and Wein MN. Springer. Third Edition, 375 (2020).

7 de Lau, W., Peng, W. C., Gros, P. & Clevers, H. The R-spondin/Lgr5/Rnf43 module: regulator of Wnt signal strength. *Genes Dev* **28**, 305-316, doi:10.1101/gad.235473.113 (2014).

8 de Lau, W. B., Snel, B. & Clevers, H. C. The R-spondin protein family. *Genome Biol* **13**, 242, doi:10.1186/gb-2012-13-3-242 (2012).

9 Knight, M. N. & Hankenson, K. D. R-spondins: novel matricellular regulators of the skeleton. *Matrix Biol* **37**, 157-161, doi:10.1016/j.matbio.2014.06.003 (2014).

10 Lu, W. *et al.* R-spondin1 synergizes with Wnt3A in inducing osteoblast differentiation and osteoprotegerin expression. *FEBS Lett* **582**, 643-650, doi:10.1016/j.febslet.2008.01.035 (2008).

11 Nagano, K. R-spondin signaling as a pivotal regulator of tissue development and homeostasis. *Jpn Dent Sci Rev* **55**, 80-87, doi:10.1016/j.jdsr.2019.03.001 (2019).

12 Raslan, A. A. & Yoon, J. K. R-spondins: Multi-mode WNT signaling regulators in adult stem cells. *Int J Biochem Cell Biol* **106**, 26-34, doi:10.1016/j.biocel.2018.11.005 (2019).

13 Shi, G. X., Mao, W. W., Zheng, X. F. & Jiang, L. S. The role of R-spondins and their receptors in bone metabolism. *Prog Biophys Mol Biol* **122**, 93-100, doi:10.1016/j.pbiomolbio.2016.05.012 (2016).

14 Glinka, A. *et al.* LGR4 and LGR5 are R-spondin receptors mediating Wnt/beta-catenin and Wnt/PCP signalling. *EMBO Rep* **12**, 1055-1061, doi:10.1038/embor.2011.175 (2011).

15 Hao, H. X. *et al.* ZNRF3 promotes Wnt receptor turnover in an R-spondin-sensitive manner. *Nature* **485**, 195-200, doi:10.1038/nature11019 (2012).

16 Ruffner, H. *et al.* R-Spondin potentiates Wnt/beta-catenin signaling through orphan receptors LGR4 and LGR5. *PLoS One* **7**, e40976, doi:10.1371/journal.pone.0040976 (2012).

17 Wang, D. *et al.* Structural basis for R-spondin recognition by LGR4/5/6 receptors. *Genes Dev* **27**, 1339-1344, doi:10.1101/gad.219360.113 (2013).

18 Xie, Y. *et al.* Interaction with both ZNRF3 and LGR4 is required for the signalling activity of R-spondin. *EMBO Rep* **14**, 1120-1126, doi:10.1038/embor.2013.167 (2013).

19 Lebensohn, A. M. & Rohatgi, R. R-spondins can potentiate WNT signaling without LGRs. *Elife* **7**, doi:10.7554/eLife.33126 (2018).

20 Szenker-Ravi, E. *et al.* RSPO2 inhibition of RNF43 and ZNRF3 governs limb development independently of LGR4/5/6. *Nature* **557**, 564-569, doi:10.1038/s41586-018-0118-y (2018).

21 Rong, X. *et al.* R-spondin 3 regulates dorsoventral and anteroposterior patterning by antagonizing Wnt/beta-catenin signaling in zebrafish embryos. *PLoS One* **9**, e99514, doi:10.1371/journal.pone.0099514 (2014).

22 Wu, C. *et al.* RSPO2-LGR5 signaling has tumour-suppressive activity in colorectal cancer. *Nat Commun* **5**, 3149, doi:10.1038/ncomms4149 (2014).

23 Lee, H., Seidl, C., Sun, R., Glinka, A. & Niehrs, C. R-spondins are BMP receptor antagonists in Xenopus early embryonic development. *Nat Commun* **11**, 5570, doi:10.1038/s41467-020-19373-w (2020).

24 Aoki, M. *et al.* R-spondin3 is required for mouse placental development. *Dev Biol* **301**, 218-226, doi:10.1016/j.ydbio.2006.08.018 (2007).

25 Neufeld, S. *et al.* A conditional allele of Rspo3 reveals redundant function of R-spondins during mouse limb development. *Genesis* **50**, 741-749, doi:10.1002/dvg.22040 (2012).

26 Ishii, Y. *et al.* Mutations in R-spondin 4 (RSPO4) underlie inherited anonychia. *J Invest Dermatol* **128**, 867-870, doi:10.1038/sj.jid.5701078 (2008).

27 Kazanskaya, O. *et al.* The Wnt signaling regulator R-spondin 3 promotes angioblast and vascular development. *Development* **135**, 3655-3664, doi:10.1242/dev.027284 (2008).

28 Knight, M. N. *et al.* R-spondin-2 is a Wnt agonist that regulates osteoblast activity and bone mass. *Bone Res* **6**, 24, doi:10.1038/s41413-018-0026-7 (2018).

29 Park, S. *et al.* Differential activities and mechanisms of the four R-spondins in potentiating Wnt/beta-catenin signaling. *J Biol Chem* **293**, 9759-9769, doi:10.1074/jbc.RA118.002743 (2018).

30 Parma, P. *et al.* R-spondin1 is essential in sex determination, skin differentiation and malignancy. *Nat Genet* **38**, 1304-1309, doi:10.1038/ng1907 (2006).

31 Wei, Q. *et al.* R-spondin1 is a high affinity ligand for LRP6 and induces LRP6 phosphorylation and beta-catenin signaling. *J Biol Chem* **282**, 15903-15911, doi:10.1074/jbc.M701927200 (2007).

32 Nam, J. S., Turcotte, T. J. & Yoon, J. K. Dynamic expression of R-spondin family genes in mouse development. *Gene Expr Patterns* **7**, 306-312, doi:10.1016/j.modgep.2006.08.006 (2007).

33 Duncan, E. L. *et al.* Genome-wide association study using extreme truncate selection identifies novel genes affecting bone mineral density and fracture risk. *PLoS Genet* **7**, e1001372, doi:10.1371/journal.pgen.1001372 (2011).

34 Estrada, K. *et al.* Genome-wide meta-analysis identifies 56 bone mineral density loci and reveals 14 loci associated with risk of fracture. *Nat Genet* **44**, 491-501, doi:10.1038/ng.2249 (2012).

35 Lee, D. Y. *et al.* Association between polymorphisms in Wnt signaling pathway genes and bone mineral density in postmenopausal Korean women. *Menopause* **17**, 1064-1070, doi:10.1097/gme.0b013e3181da4da3 (2010).

36 Medina-Gomez, C. *et al.* Meta-analysis of genome-wide scans for total body BMD in children and adults reveals allelic heterogeneity and age-specific effects at the WNT16 locus. *PLoS Genet* **8**, e1002718, doi:10.1371/journal.pgen.1002718 (2012).

37 Richards, J. B. *et al.* Bone mineral density, osteoporosis, and osteoporotic fractures: a genome-wide association study. *Lancet* **371**, 1505-1512, doi:10.1016/S0140-6736(08)60599-1 (2008).

38 Richards, J. B., Zheng, H. F. & Spector, T. D. Genetics of osteoporosis from genome-wide association studies: advances and challenges. *Nat Rev Genet* **13**, 576-588, doi:10.1038/nrg3228 (2012).

39 Zhu, C. *et al.* LGR4 acts as a key receptor for R-spondin 2 to promote osteogenesis through Wnt signaling pathway. *Cell Signal* **28**, 989-1000, doi:10.1016/j.cellsig.2016.04.010 (2016).

40 Zhang, M. *et al.* RSPO3-LGR4 Regulates Osteogenic Differentiation Of Human Adipose-Derived Stem Cells Via ERK/FGF Signalling. *Sci Rep* **7**, 42841, doi:10.1038/srep42841 (2017).

41 Schepers, K. *et al.* Myeloproliferative neoplasia remodels the endosteal bone marrow niche into a self-reinforcing leukemic niche. *Cell Stem Cell* **13**, 285-299, doi:10.1016/j.stem.2013.06.009 (2013).

42 Rauch, A. *et al.* Glucocorticoids suppress bone formation by attenuating osteoblast differentiation via the monomeric glucocorticoid receptor. *Cell Metab* **11**, 517-531, doi:10.1016/j.cmet.2010.05.005 (2010).

43 Li, J. *et al.* Dkk1-mediated inhibition of Wnt signaling in bone results in osteopenia. *Bone* **39**, 754-766, doi:10.1016/j.bone.2006.03.017 (2006).

44 Zhou, Q. *et al.* ERK signaling is a central regulator for BMP-4 dependent capillary sprouting. *Cardiovasc Res* **76**, 390-399, doi:10.1016/j.cardiores.2007.08.003 (2007).

45 Cervenka, I. *et al.* Mitogen-activated protein kinases promote WNT/beta-catenin signaling via phosphorylation of LRP6. *Mol Cell Biol* **31**, 179-189, doi:10.1128/MCB.00550-10 (2011).

46 Gortazar, A. R., Martin-Millan, M., Bravo, B., Plotkin, L. I. & Bellido, T. Crosstalk between caveolin-1/extracellular signal-regulated kinase (ERK) and beta-catenin survival pathways in osteocyte mechanotransduction. *J Biol Chem* **288**, 8168-8175, doi:10.1074/jbc.M112.437921 (2013).

47 Kim, J. M. *et al.* The ERK MAPK Pathway Is Essential for Skeletal Development and Homeostasis. *Int J Mol Sci* **20**, doi:10.3390/ijms20081803 (2019).

48 Krejci, P. *et al.* Receptor tyrosine kinases activate canonical WNT/beta-catenin signaling via MAP kinase/LRP6 pathway and direct beta-catenin phosphorylation. *PLoS One* **7**, e35826, doi:10.1371/journal.pone.0035826 (2012).

49 Yoon, J. K. & Lee, J. S. Cellular signaling and biological functions of R-spondins. *Cell Signal* **24**, 369-377, doi:10.1016/j.cellsig.2011.09.023 (2012).

50 Azzolin, L. *et al.* YAP/TAZ incorporation in the beta-catenin destruction complex orchestrates the Wnt response. *Cell* **158**, 157-170, doi:10.1016/j.cell.2014.06.013 (2014).

51 de Lau, W. *et al.* Lgr5 homologues associate with Wnt receptors and mediate R-spondin signalling. *Nature* **476**, 293-297, doi:10.1038/nature10337 (2011).

52 Luo, J. *et al.* Regulation of bone formation and remodeling by G-protein-coupled receptor 48. *Development* **136**, 2747-2756, doi:10.1242/dev.033571 (2009).

53 Xu, P. *et al.* Lgr4 is crucial for skin carcinogenesis by regulating MEK/ERK and Wnt/beta-catenin signaling pathways. *Cancer Lett* **383**, 161-170, doi:10.1016/j.canlet.2016.09.005 (2016).

54 Lin, W. *et al.* Lgr5-overexpressing mesenchymal stem cells augment fracture healing through regulation of Wnt/ERK signaling pathways and mitochondrial dynamics. *FASEB J* **33**, 8565-8577, doi:10.1096/fj.201900082RR (2019).

55 Vieira, G. C. *et al.* LGR5 regulates pro-survival MEK/ERK and proliferative Wnt/beta-catenin signalling in neuroblastoma. *Oncotarget* **6**, 40053-40067, doi:10.18632/oncotarget.5548 (2015).

56 Kamiya, N. *et al.* Targeted disruption of BMP signaling through type IA receptor (BMPR1A) in osteocyte suppresses SOST and RANKL, leading to dramatic increase in bone mass, bone mineral density and mechanical strength. *Bone* **91**, 53-63, doi:10.1016/j.bone.2016.07.002 (2016).

57 Simsek Kiper, P. O. *et al.* Cortical-Bone Fragility--Insights from sFRP4 Deficiency in Pyle's Disease. *N Engl J Med* **374**, 2553-2562, doi:10.1056/NEJMoa1509342 (2016).

58 Kamiya, N. *et al.* Wnt inhibitors Dkk1 and Sost are downstream targets of BMP signaling through the type IA receptor (BMPRIA) in osteoblasts. *J Bone Miner Res* **25**, 200-210, doi:10.1359/jbmr.090806 (2010).

59 Kamiya, N. *et al.* BMP signaling negatively regulates bone mass through sclerostin by inhibiting the canonical Wnt pathway. *Development* **135**, 3801-3811, doi:10.1242/dev.025825 (2008).

60 Ko, F. C. *et al.* Treatment With a Soluble Bone Morphogenetic Protein Type 1A Receptor (BMPR1A) Fusion Protein Increases Bone Mass and Bone Formation in Mice Subjected to Hindlimb Unloading. *JBMR Plus* **1**, 66-72, doi:10.1002/jbm4.10012 (2017).

61 Shi, C. *et al.* Bone morphogenetic protein signaling through ACVR1 and BMPR1A negatively regulates bone mass along with alterations in bone composition. *J Struct Biol* **201**, 237-246, doi:10.1016/j.jsb.2017.11.010 (2018).

62 Dempster, D. W. *et al.* Standardized nomenclature, symbols, and units for bone histomorphometry: a 2012 update of the report of the ASBMR Histomorphometry Nomenclature Committee. *J Bone Miner Res* **28**, 2-17, doi:10.1002/jbmr.1805 (2013).

63 Chen, K. *et al.* Sfrp4 repression of the Ror2/Jnk cascade in osteoclasts protects cortical bone from excessive endosteal resorption. *Proc Natl Acad Sci U S A* **116**, 14138-14143, doi:10.1073/pnas.1900881116 (2019).

64 Moverare-Skrtic, S. *et al.* Osteoblast-derived WNT16 represses osteoclastogenesis and prevents cortical bone fragility fractures. *Nat Med* **20**, 1279-1288, doi:10.1038/nm.3654 (2014).

65 Livak, K. J. & Schmittgen, T. D. Analysis of relative gene expression data using real-time quantitative PCR and the 2(-Delta Delta C(T)) Method. *Methods* **25**, 402-408, doi:10.1006/meth.2001.1262 (2001).

Acknowledgments

This work was supported by NIH-NIAMS R01AR064724 to R.B.

Author contributions

F.G. and R.B. conception of the work; K.N., K.Y., F.G. and R.B. design of the work; F.G. and R.B. supervised the project; K.N., K.Y., H.S., R.K., A.C.P and D.R. acquisition and analysis of data; K.N., K.Y., F.G. and R.B. interpretation of data; F.G. and R.B. wrote the paper, K.N. and C.N. contributed to the writing and revision of the paper.

Competing interest statements

The Authors do not have competing interest.

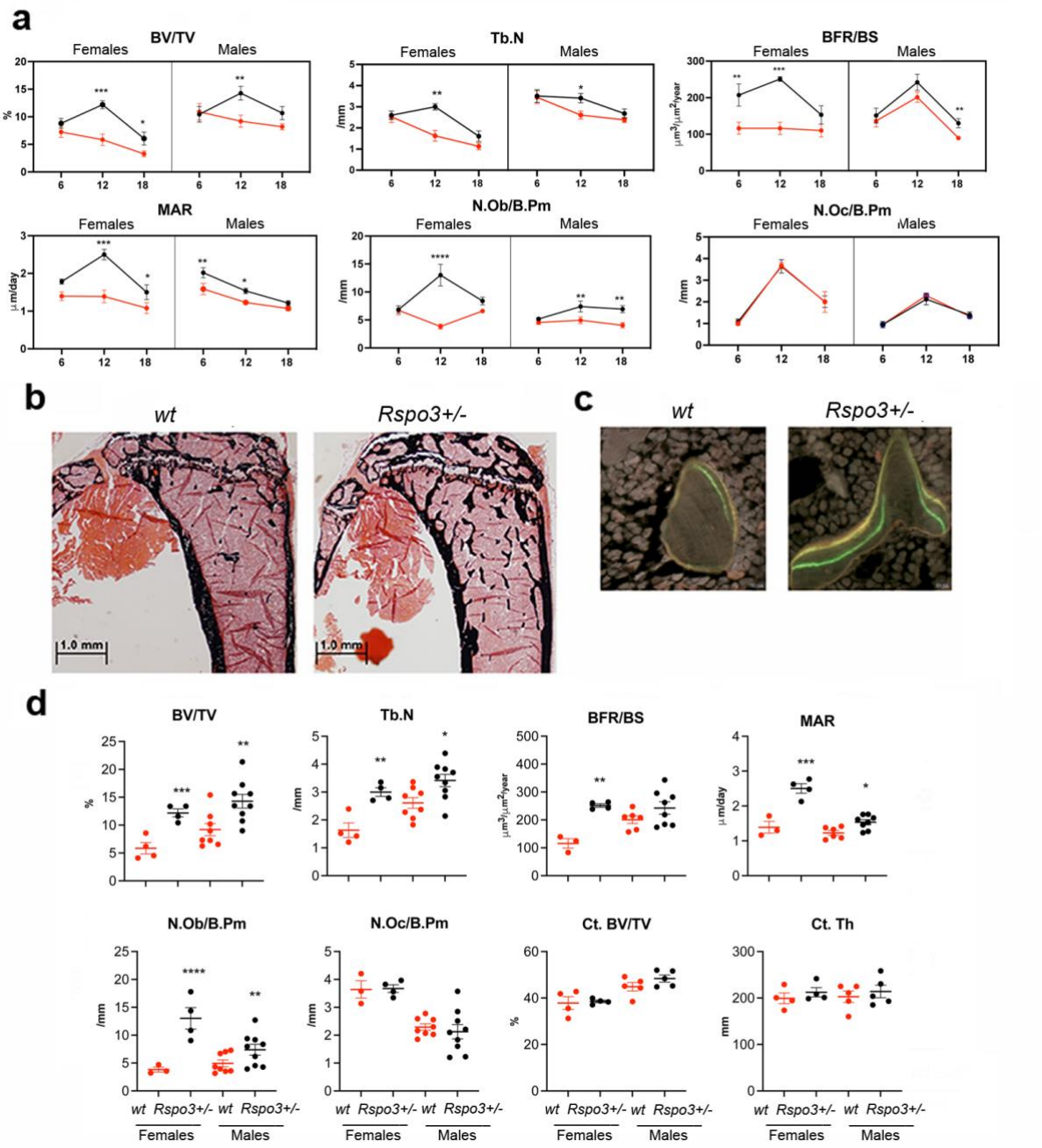

Figure 1. Skeletal phenotype of mice with *Rspo3* haplo-insufficiency. **a**) Histomorphometric analysis at 6-, 12- and 18-wk male and female mice (n=4-9). Data are the mean ± SEM. Two Way ANOVA followed by Fisher's LSD test.*p<0.05, **p<0.005, ****p<0.0001. **b-c**) Representative images of Von Kossa staining (b) and trabecular MAR (c) in 12 wk-old *wt* and *Rspo3*$^{+/-}$ male tibiae. **d**) Histomorphometric analysis of 12 wk-old *wt* and *Rspo3*$^{+/-}$ female and male tibiae (n=4-9). Data show all samples and the mean ± SEM. *=p<0.05, **p<0.005 by Student T-test.

Table 1. Histomorphometric analysis of *Rspo3*$^{+/-}$ and *wt* females.

Parameters	6 wk		12 wk		18 wk		Two Way ANOVA		
	wt (n=6)	*Rspo3*$^{+/-}$ (n=7)	*wt* (n=4)	*Rspo3*$^{+/-}$ (n=4)	*wt* (n=8)	*Rspo3*$^{+/-}$ (n=6)	Genotype	Age	Interaction
BV/TV (%)	7.24±0.98	8.8±0.88	5.84±1.01	12.2±0.72***	3.28±0.51	6.06±1.1*	<0.0001	<0.0001	NS
Tb.Th (μm)	28.3±0.91	33.6±1.5*	35.8±2.54	40.7±1.31	28.2±1.55	36.8±2.7**	0.0003	0.0032	NS
Tb.N (/mm)	2.53±0.27	2.6±0.20	1.63±0.26	3.00±0.15**	1.13±0.16	1.61±0.25	0.0025	<0.0001	0.0429
Tb.Sp (μm)	397±52.6	368±26.4	618±86.8	297±17.1*	1050±192	690±133	0.0378	0.0008	NS
MAR (μm/day)	1.4±0.11	1.8±0.06	1.39±0.17	2.5±0.14***	1.08±0.15	1.5±0.20*	<0.0001	0.0016	NS
MS/BS (%)	22.2±2.06	31.4±4.05*	23.0±3.25	27.8±1.63	26.8±1.90	27.3±1.55	0.0394	NS	NS
BFR/BS ($\mu m^3/\mu m^2$/year)	116.2±16.6	207±30.4**	116±16.9	251±6.43**	110±17.6	153±25.1	<0.0001	NS	NS
N.Ob/B.Pm (/mm)	6.72±0.79	6.85±0.64	3.83±0.45	13±1.94****	6.60±0.39	8.4±0.69	<0.0001	NS	0.0001
Ob.S/B.Pm (%)	10.3±1.20	10.5±1.44	4.89±0.38	16.3±2.2****	9.66±0.52	12.3±0.53	<0.0001	NS	0.0007
OS/BS (%)	4.68±0.78	5.51±1.23	2.51±0.30	9.17±0.77***	4.84±0.66	8.3±0.74**	<0.0001	NS	0.0263
O.Th (μm)	3.89±0.30	4.64±0.37	2.76±0.13	4.36±0.09*	2.78±0.37	4.24±0.3**	0.0003	NS	NS
N.Oc/B.Pm (/mm)	1.08±0.13	0.99±0.11	3.64±0.31	3.67±0.14	2.01±0.26	2±0.48	NS	<0.0001	NS
Oc.S/B.Pm (%)	2.98±0.40	3.07±0.37	7.89±0.42	8.77±0.55	5.85±0.86	5.7±1.17	NS	<0.0001	NS
ES/BS (%)	4.41±1.06	4.05±0.42	1.67±0.48	2.96±0.43	6.85±0.82	6.74±1.28	NS	<0.0001	NS

Data are expressed as Mean±SEM. Two Way ANOVA followed by Fisher's LSD post-hoc test.
*=p<0.05, **=p<0.005, ***=p<0.001 , ****=p<0.0001 compared to age-matched *wt* females.

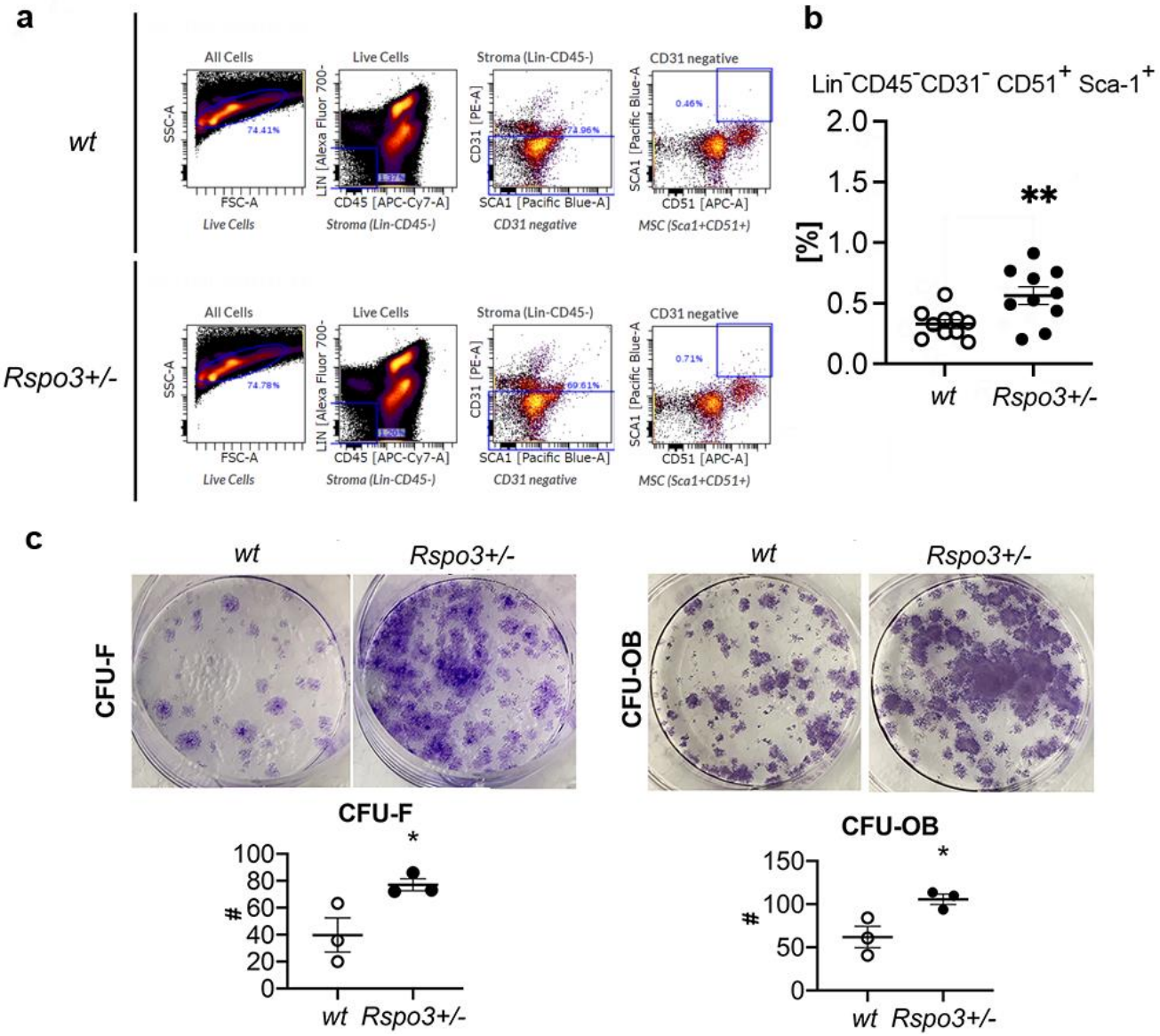

Figure 2. *Rspo3* haplo-insufficiency increases the % of osteoprogenitors. **a**) Representative images of FACS analysis. **b**) Quantification of the % of Lin$^-$Cd45$^-$Cd31$^-$CD51$^+$Sca$^+$ cells in *wt* and *Rspo3*$^{+/-}$ bone marrow. Data show all samples and the mean ± SEM (n=10) *p<0.05 by Student T-test. **c**) Representative images of CFU-F and CFU-OB and quantification in *wt* and *Rspo3*$^{+/-}$ mice. Data show all samples and the mean ± SEM (n=3) *p<0.05 by Student T-test.

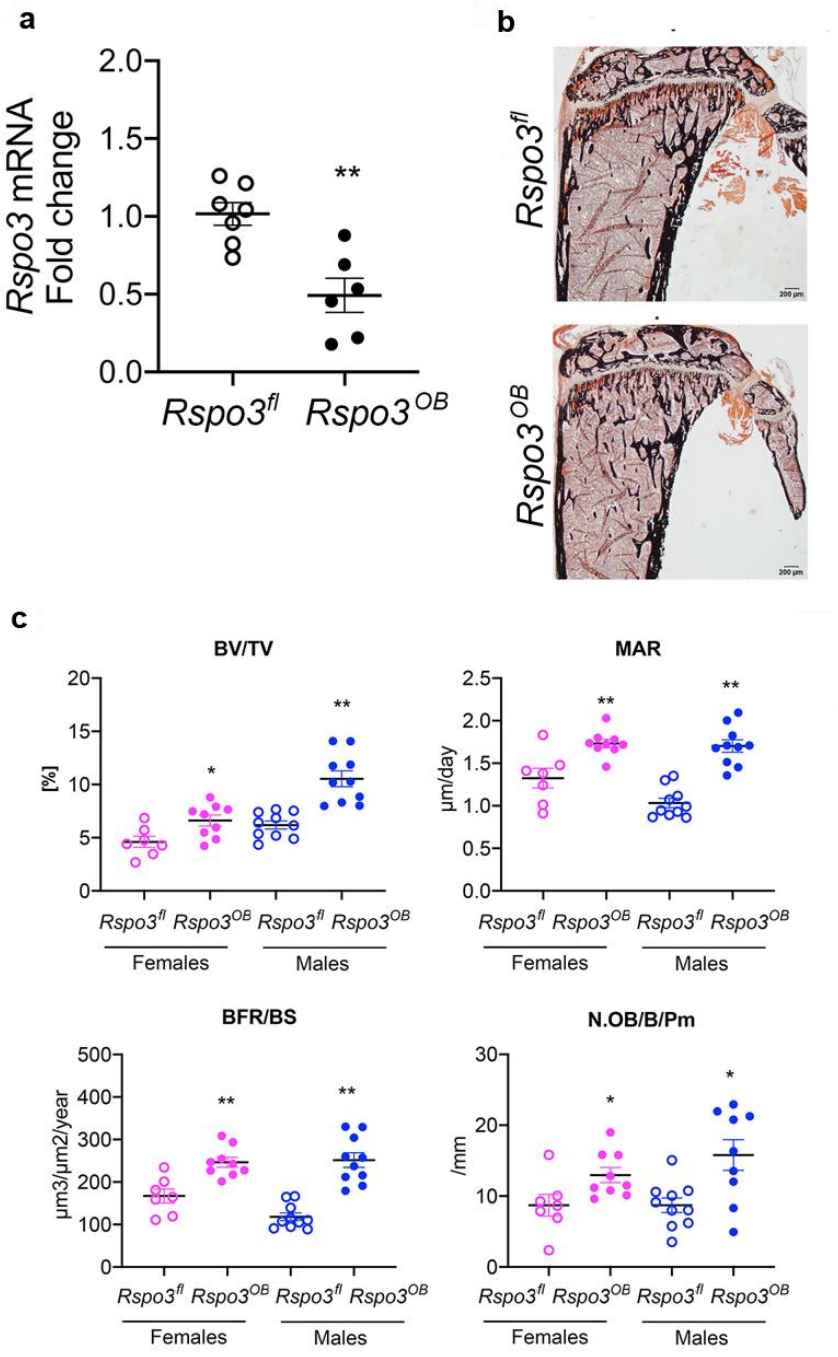

Figure 3. Skeletal phenotype of mice with *Rspo3* targeted deletion in Runx+ cells (Rspo3^{OB}). **a**) *Rspo3* expression in marrow depleted long bones (n=6-7). Data show all samples and are the mean ± SEM *= p<0.05 by Student T-test. **b**) Representative images of Von Kossa staining in 8-wk old *Rspo3^{fl}* and *Rspo3^{OB}* tibiae. **c**) BV/TV, MAR, BFR/BS and N.OB/Pm by histomorphometric analysis Rspo3^{fl} and Rspo3^{OB} females and males (n= 7-10). Data show all samples and the mean ± SEM *= p<0.05, **=p<0.005 compared to the correspondent *Rspo3^{fl}* by Student T-test.

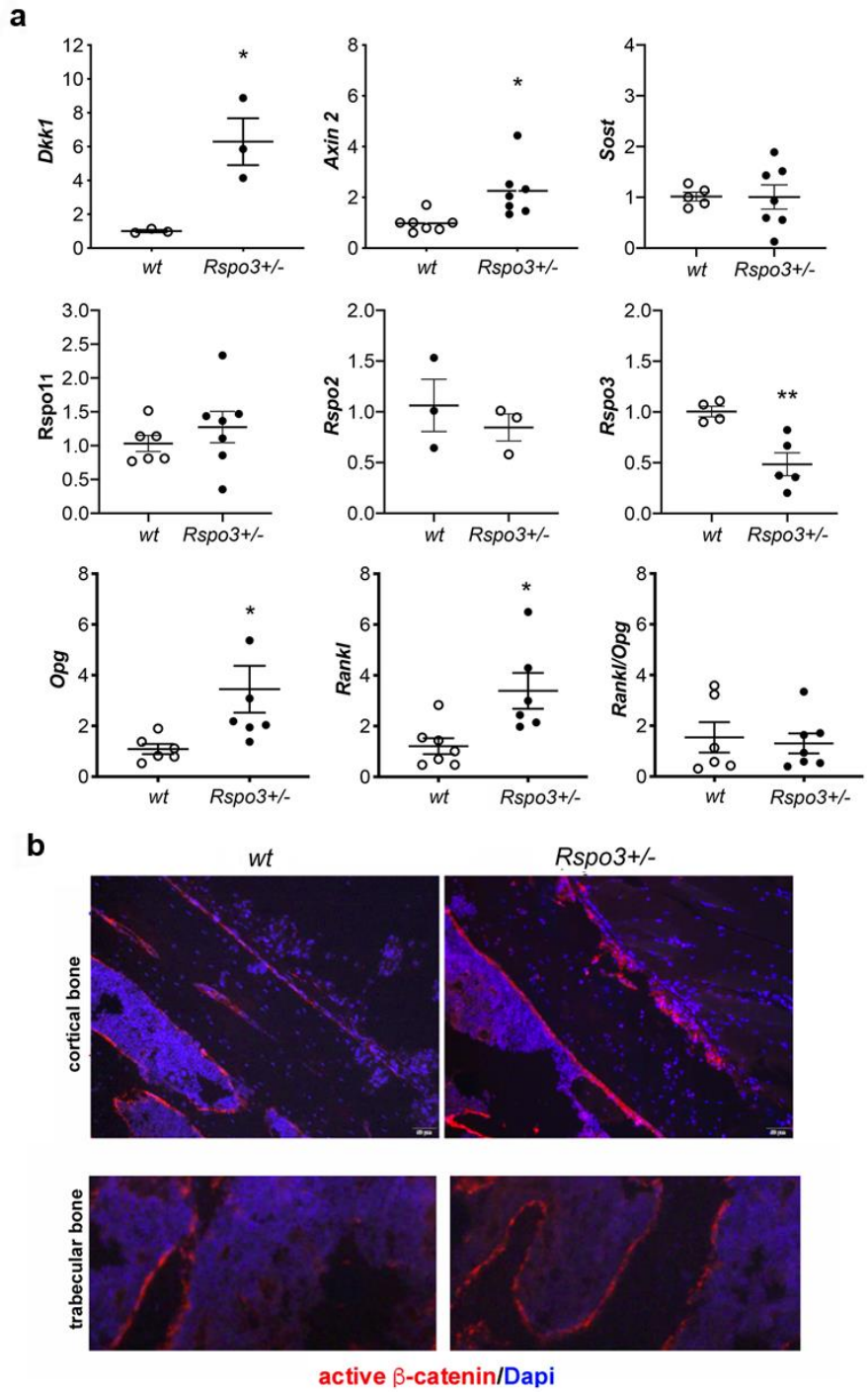

Figure 4. *Rspo3* haplo-insufficiency leads to Wnt signaling activation *in vivo*. **a**) Expression of Wnt target genes in marrow-depleted long bones (n=3-7). Data show all samples and the mean ± SEM *p<0.05 by Student T-test. **b**) Immunohistochemistry representative images of active β-catenin in the long bones of *wt* and *Rspo3*$^{+/-}$ mice.

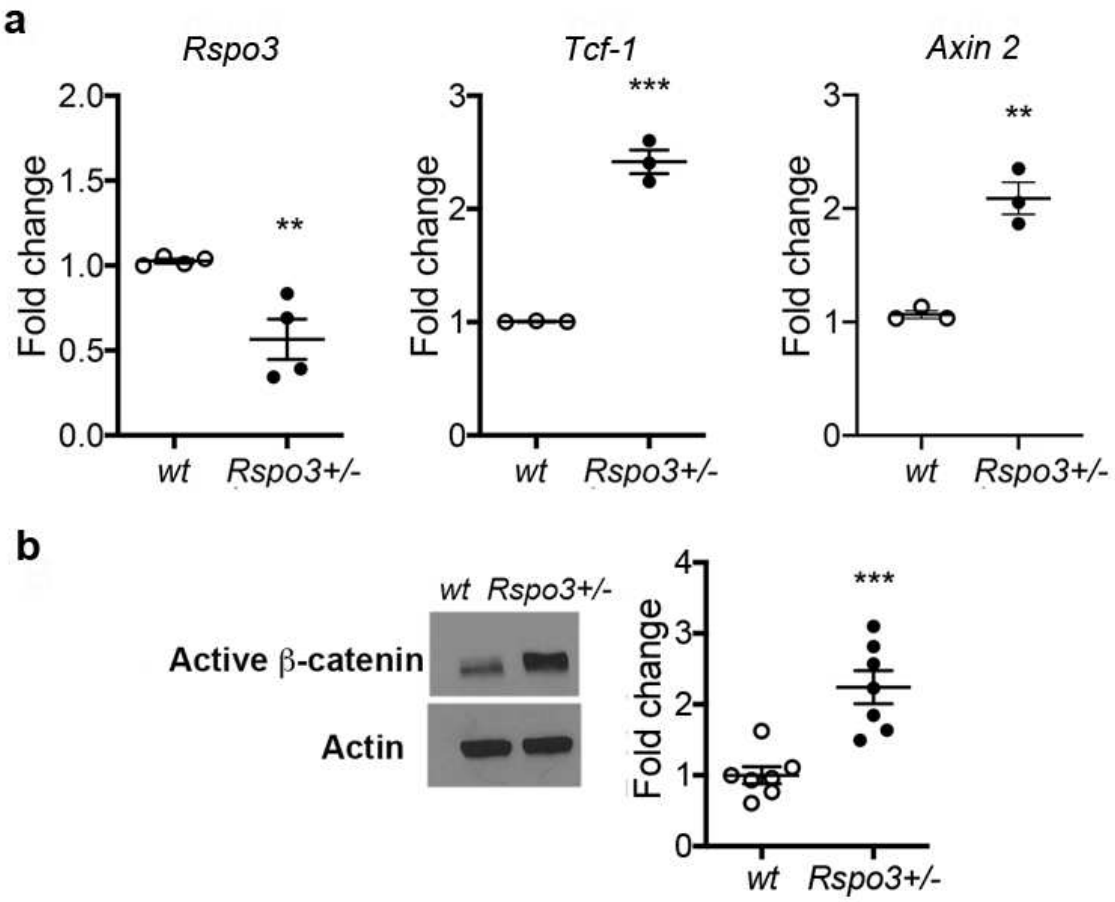

Figure 5. *Rspo3* haplo-insufficiency leads to Wnt signaling activation *in vitro*. **a**) Expression of Wnt target genes in BMSCs (n=3-4). Data show all samples and the mean ± SEM. **b**) Representative images and quantification of active β-catenin by Western analysis in BMSC isolated from *wt* and *Rspo3*$^{+/-}$ mice (n=7) **p<0.05, ***p<0.005 by Student T-test.

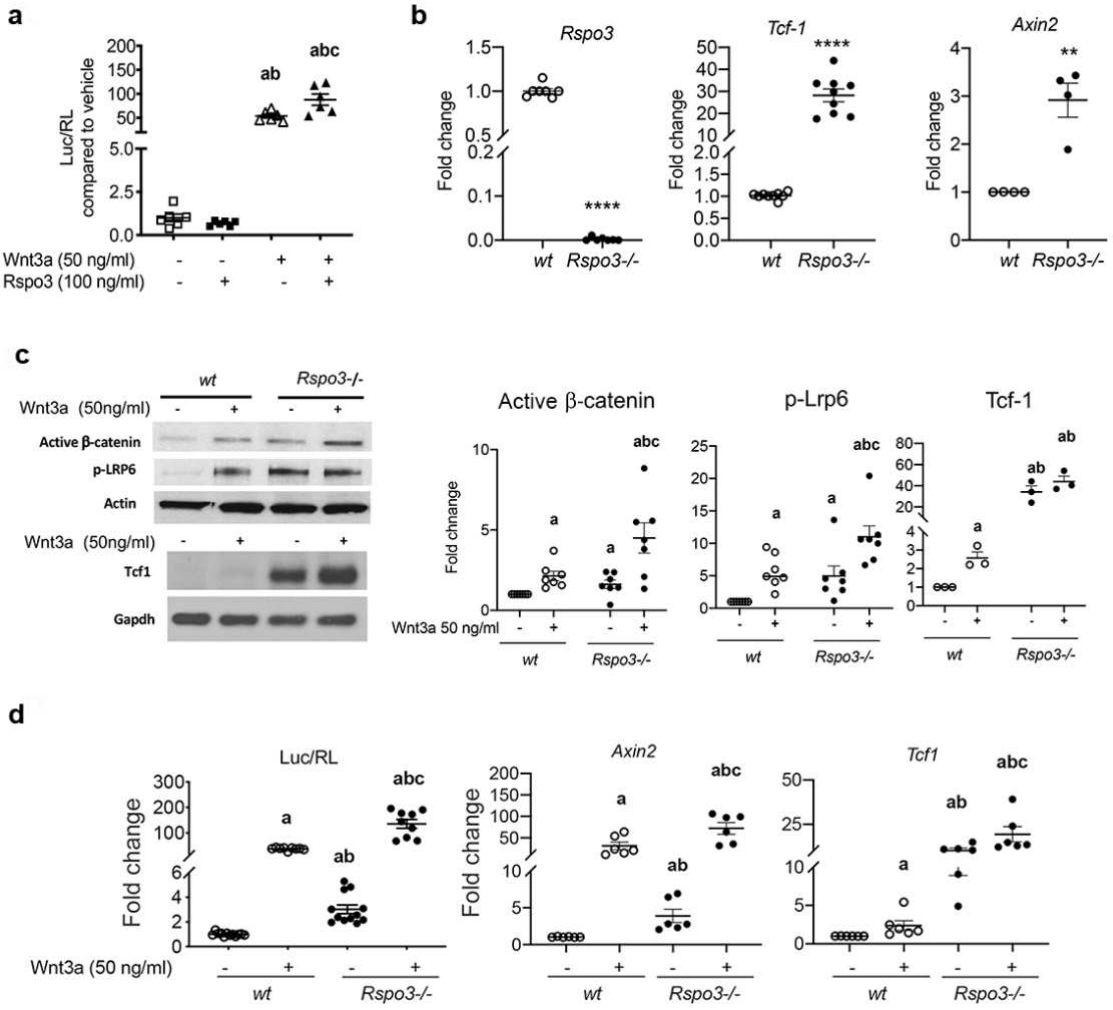

Figure 6. *Rspo3* deletion leads to Wnt signaling activation *in vitro*. **a**) Luciferase assay in *wt* MEFs treated w/wo Wnt3a and Rspo3 (n=5). Data show all samples and the mean ± SEM, a=p<0.05 vs vehicle wt, b=p<0.05 vs Rspo3 treated wt and c= p<0.05 vs Wnt3a treated wt by Two-Way ANOVA followed by Fisher's LSD test. **b**) Expression of Wnt target genes in *wt* and *Rspo*$^{-/-}$ MEFS (n=3-9). Data show all samples and the mean ± SEM.**p<0.05, ****p<0.005 by Student T-test. **c**) Representative images and quantification of active β–catenin, pLrp6 and Tcf-1 by Western analysis in *wt* and *Rspo*$^{-/-}$ MEFs treated w/wo Wnt3a (n=3-7). Data show all samples and the mean ± SEM. **d**) Luciferase assay and Wnt target gene expression in *wt* and *Rspo*$^{-/-}$ MEFs treated w/wo Wnt3a (n=6-11). Data show all samples and the mean ± SEM a=p<0.05 vs vehicle *wt*, b=p<0.05 vs Wnt3a–treated *wt* and c= p<0.05 vs Wnt3a treated *Rspo3*$^{-/-}$ by Two-Way ANOVA followed by Fisher's LSD test.

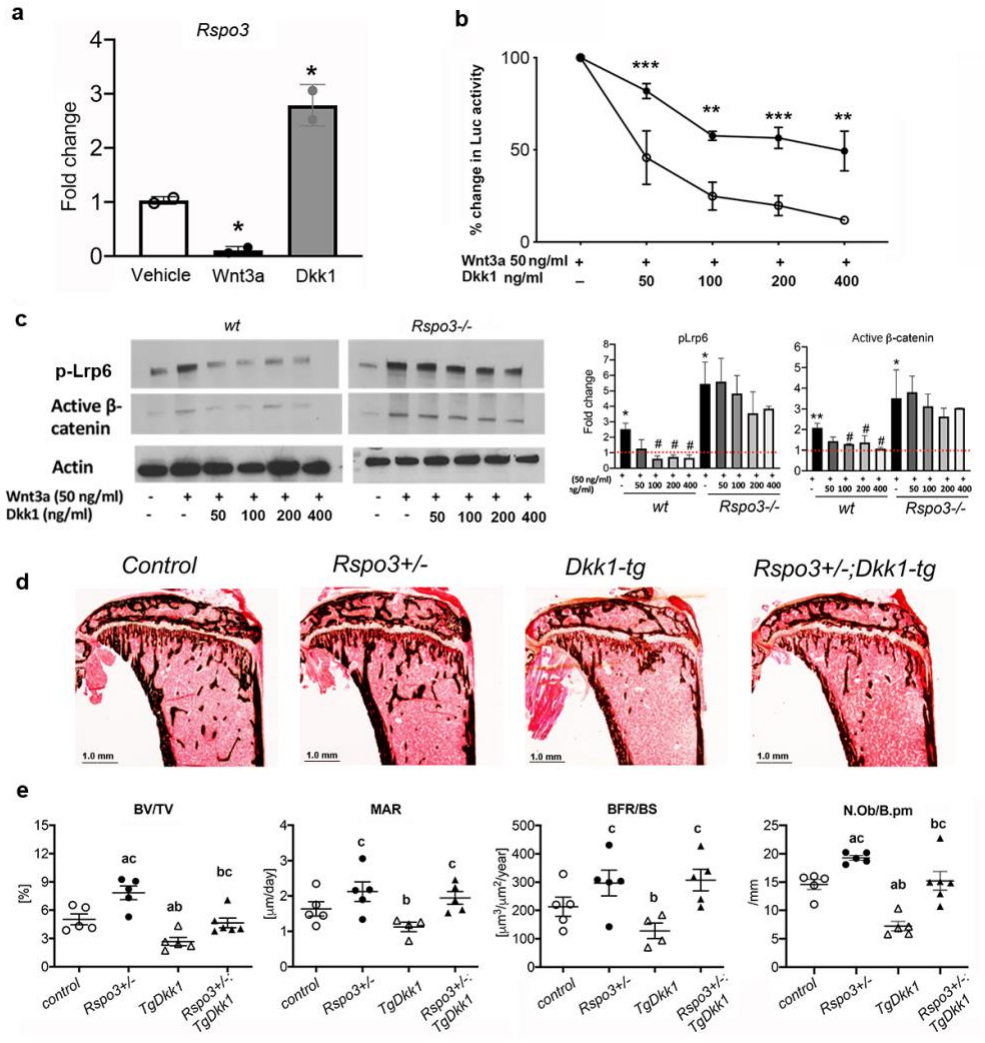

Figure 7. *Rspo3* deletion/ haplo-insufficiency impairs Dkk1 efficacy. **a**) regulation of Rspo3 by Wnt3a and Dkk1 in wt MEFs (n=2) Data are the mean ± SD. *p<0.05 . **b**) Luciferase assay in *wt* and *Rspo*$^{-/-}$ MEFs treated w/wo Wnt3a and increasing doses of Dkk1 (n=3-4). Data are the mean ± SEM **p<0.005, ***<p<0.0005 compared to vehicle same genotype by Student-t test. **c**) Representative images and quantification of active β-catenin and pLrp6 by Western analysis in *wt* and *Rspo3*$^{-/-}$ MEFs treated w/wo Wnt3a and increasing doses of Dkk1 (n=3). Data are the mean ± SEM *p<0.05, **p,0.005 vs wt vehicle, # = vs Wnt3a–treated same genotype by Student-t test. **d**) Representative images of Von Kossa staining in 6-wk old female mice. **e**) BV/TV, MAR, BFR/BS and N.Ob./B.pm by histomorphometric analysis in females (n= 5-6). Data show all samples and the mean ± SEM a=p<0.05 compared to *control* mice, b= p<0.05 compared to *Rspo3*$^{+/-}$ mice, c= p<0.05 compared to *Dkk1-Tg* mice by two-Way ANOVA followed by Fisher's LSD test.

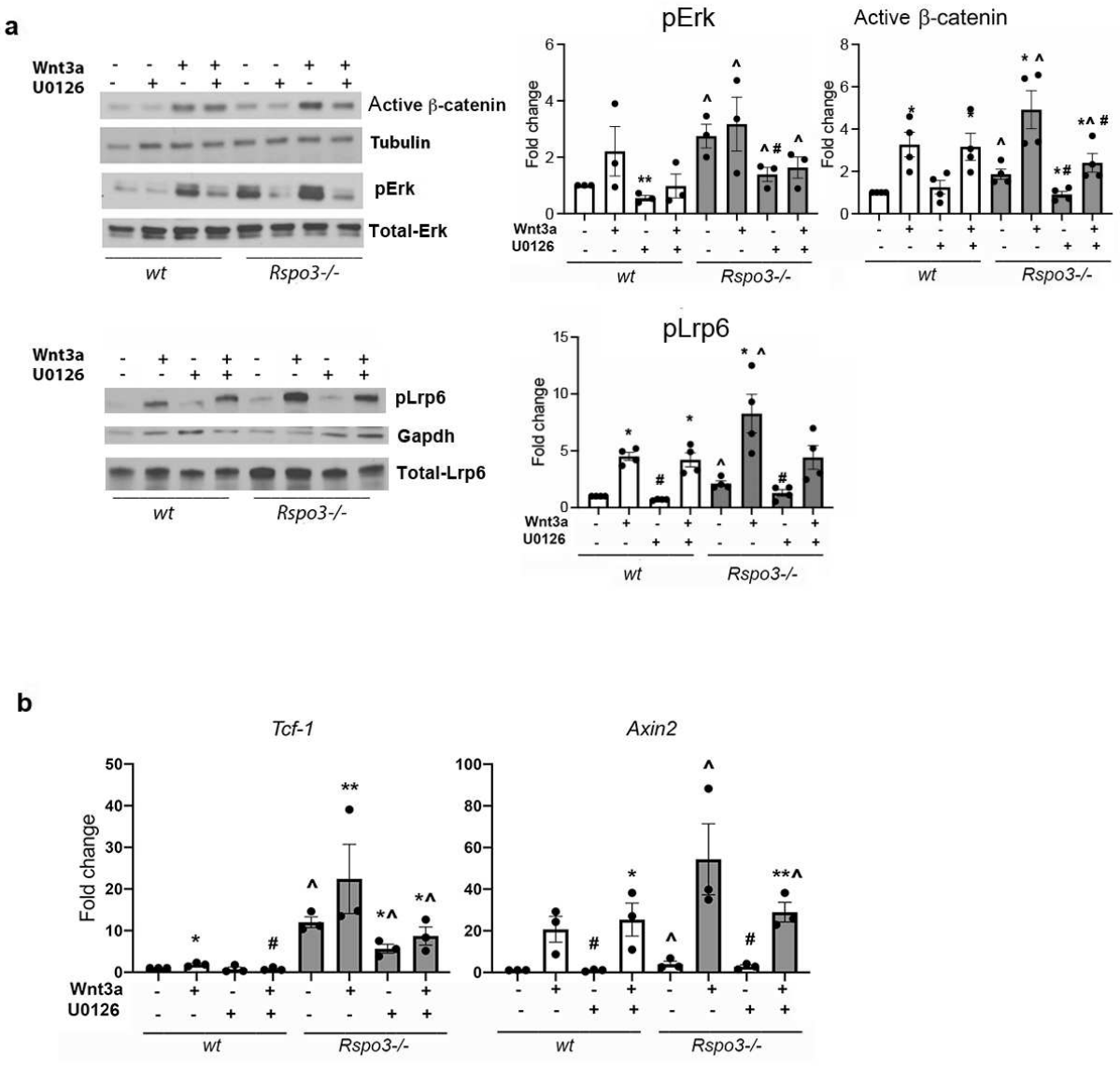

Figure 8. Erk signaling is involved in the Wnt signaling activation seen in the absence of Rspo3. **a**) Representative images and quantification of pERK, active β-catenin and pLrp6 by western analysis in *wt* and *Rspo3*$^{-/-}$ MEFs treated w/wo w/wo Wnt3a and U0126. **b**) Expression of Wnt target genes in *wt* and *Rspo3*$^{-/-}$ MEFs treated w/wo Wnt3a and U0126. Data show all samples and the mean $\pm$ SEM (n=3-4) *p<0.05, **p,0.005 vs vehicle of the same genotype, ^ = p<0.05 vs wt vehicle and # = p<0.05 vs Wnt3a–treated same genotype by Student-t test.

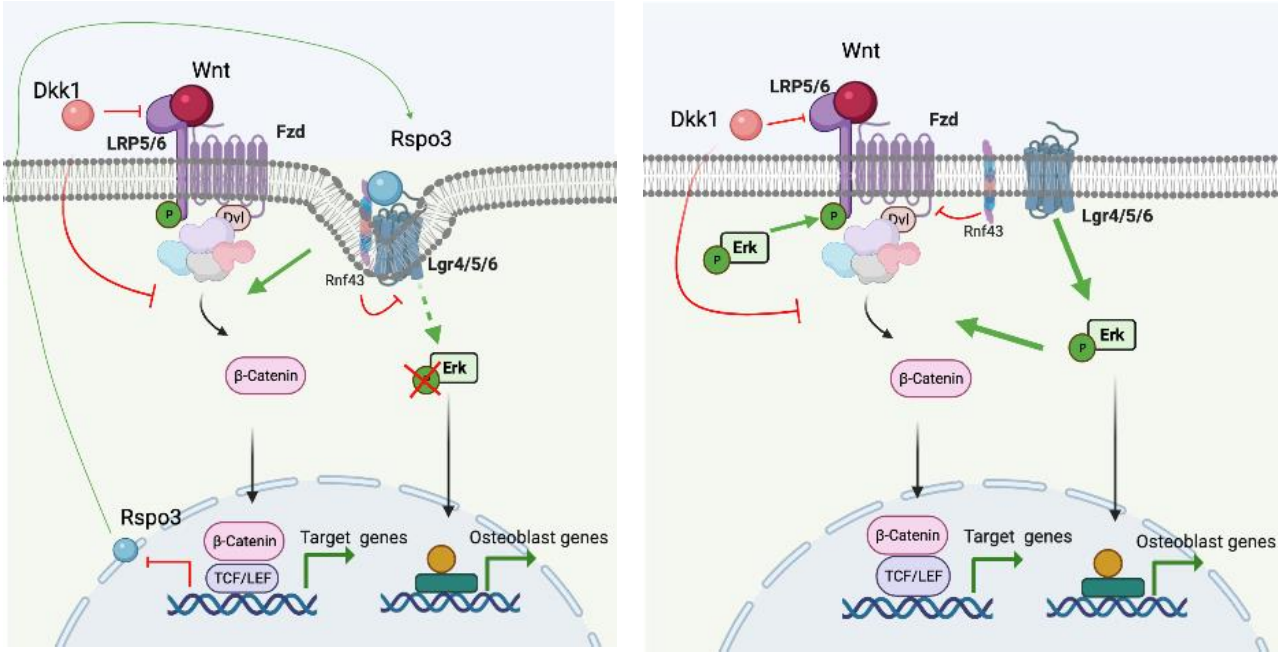

Figure 9. Proposed model. Rspo3 has a dual mode of action to regulate canonical Wnt signaling and thereby bone formation. This duality is based on the regulation of two distinct signaling cascades and their crosstalk: Rspo3 functions via both the Lgr/Rnf43/Znrf3 and the Lgr/Erk axes. In the presence of Rspo3, the Rspo3/Lgr/Rnf43/Znrf3 axis boosts Wnt signaling strengths by the membrane clearance of Rnf43/Znrf3 and subsequent stabilization of Fzd receptors. In addition, binding of Rspo3 to Lgr impairs Erk signaling likely due to the membrane clearance of the Lgr/Rnf43/Znrf3 receptors, preventing Erk signaling activation. Deletion of Rspo3 would dampen Wnt signaling at the cell surface by preventing the Rnf43/Znrf3 effects while promoting Erk activation downstream of Lgr receptors in turn enhancing Lrp5/6 phosphorylation and β–catenin stabilization intracellularly, which has a more potent effect and overcompensates the decrease in Rspo3-dependent proximal Wnt activation in osteoblasts and their progenitors. Figure created with Biorender.

Supplementary Files

This is a list of supplementary files associated with this preprint. Click to download.

- GoriBaronSupplementarydocs.pdf